Co-generation of Ammonia and H$_2$ from H$_2$O Vapor and N$_2$ Using a Membrane Electrode Assembly

Kurt Kugler[1], Stefanie M. A. Kriescher[1], Martin Giela[1], Schwan Hosseiny[1], Kristof Thimm[1], and Matthias Wessling[1,2,*]

Supporting Information available online

The direct electrochemical synthesis of NH$_3$ from nitrogen and water vapor without the use of a fossil carbon source is highly desired. This synthesis is a viable option to store energy and produce fertilizer precursors. Here, a new Pt-free membrane electrode assembly is presented. An electrochemical membrane reactor demonstrates the feasibility of co-generating NH$_3$ and H$_2$ directly from nitrogen and water vapor at ambient conditions. An unprecedented high NH$_3$-specific current efficiency of up to 27.5% using Ti as cathodic catalyst is reported. The co-generation can be tuned by the balance of process parameters.

1 Introduction

The most important chemical process invention of the 20th century is the Haber process for NH$_3$ production [1]. At 400 to 500 °C and 150 to 200 bar, N$_2$ and H$_2$ react to form NH$_3$. The required H$_2$ is produced by the reformation of CH$_4$ or coal with H$_2$O. It would be highly desirable to omit the use of carbon sources for H$_2$ production. Additionally, for each ton of NH$_3$ produced, approximately 2 t CO$_2$ are emitted. [2] Elimination of this CO$_2$ emission is also highly desired.

Ammonia is a colorless and poisonous gas. Around 80 % of the produced NH$_3$ is converted to be used as fertilizer. Recently, Wang et al. proposed an ammonia-based energy storage system [3]. NH$_3$ may also become an important intermediate chemical for energy and indirect H$_2$ storage [4, 5]. In fact, Lan and Tao used (NH$_4$)$_2$CO$_3$ in fuel cell applications [6]. Water electrolysis in a proton exchange membrane (PEM) electrolyzer is a well-developed process for sustainable H$_2$ production [7]. The transportation and storage of gaseous H$_2$ are more challenging than for liquid NH$_3$ [8].

A potentially more sustainable NH$_3$ synthesis method is proposed by the direct reduction of N$_2$ using an electrochemical membrane reactor (ecMR) [9]. As opposed to the Haber process, the emission of the greenhouse gas CO$_2$ is avoided, since renewable energy sources such as wind or solar power are applied to power the process.

An ecMR has a similar architecture as a PEM electrolyzer: it comprises an anode performing water oxidation, a PEM, and a cathode conducting the desired reduction as well as parallel reactions. The feasibility of the ecMR for the electrochemical reduction of CO$_2$ to synthesize hydrocarbons was proved [10], however at very low production rates and current efficiencies. Here, the concept of an ecMR process for simultaneous NH$_3$ and H$_2$ generation is proposed. The process is carbon-independent and CO$_2$-free: H$_2$O is used as an abundant source of H$_2$, and renewable energy can potentially drive the reaction.

Recently, Nash et al. [11] investigated NH$_3$ synthesis by using a membrane electrode assembly (MEA) consisting of a PEM or a hydroxide exchange membrane containing a noble metal cathode. Furthermore, Yang et al. [12] used a cathode containing vanadium nitride nanoparticles loaded on carbon paper hot-pressed on a Pt/C-coated (anode) Nafion membrane. However, both studies used H$_2$ as proton source. To overcome the additional H$_2$ production step, H$_2$O is used as proton source in this study and by Lan et al.

[1]Dr.-Ing. Kurt Kugler, Dr.-Ing. Stefanie M. A. Kriescher, Martin Giela, Dr.-Ing. Schwan Hosseiny, Kristof Thimm, Prof. Dr.-Ing. Matthias Wessling
manuscripts.cvt@avt.rwth-aachen.de
RWTH Aachen University, Chemical Process Engineering, Forckenbeckstraße 51, 52074 Aachen, Germany.
[2]Prof. Dr.-Ing. Matthias Wessling
DWI – Leibniz Institute for Interactive Materials, Forckenbeckstraße 50, 52074 Aachen, Germany.

[13]. Nonetheless, Lan et al. [13] described a comparable system with the major difference to the new process reported here being (i) that the H_2O vapor phase used here allows the control of the H_2O vapor activity at the anode side by varying molar H_2O fraction and (ii) that our MEA is Pt-free and the cathode is based on abundant Ti.

1.1 Membrane Electrode Assembly

The core of the ecMR is the MEA, which combines (i) the oxygen evolution reaction (OER) at the anode, (ii) the migration of H^+ ions across the polymer cation exchange membrane (CEM), and (iii) the reduction of N_2 to NH_3 at the cathode (Fig. 1a). The main (parallel) reaction at the cathode is a reduction of H^+, i.e., the hydrogen evolution reaction (HER). The MEA presented here consisted of three elements: a) an iridium mixed metal oxide (IrMMO) anode, b) a polymer CEM, and c) a Ti cathode responsible for N_2 reduction.

As indicated in previous work [9], we assume that a cryogenic air separation needs to be applied before the electrochemical NH_3 synthesis process, to separate O_2 from N_2 and to produce pure N_2. Further research has to be carried out to investigate to what extent the assumption of pure N_2 can be released and O_2 may be present in the feed gas. In fact, it may be reduced to H_2O again depending on the potentials applied.

Ir and IrO_2 are the preferred species for the OER. A mixture of IrO_2 and Ta_2O_5 (at a 70/30 ratio) is known to be the most active and most stable composition. In the mixed metal oxide catalyst, IrO_2 is the active species for the OER, while Ta_2O_5 stabilizes the catalyst and retards the reduction of IrO_2 to the less active Ir. [14]

The H^+ ions formed at the IrMMO anode migrate through a perfluorosulfonic acid-based PEM (Fig. 1b). The conductivity of the polymer membranes depends mainly on the temperature and the relative humidity at which the membrane is operated [15]. Protons carry H_2O molecules through electro-osmosis: such H_2O transport needs to be balanced well as developed for water management strategies in H_2 fuel cells [16].
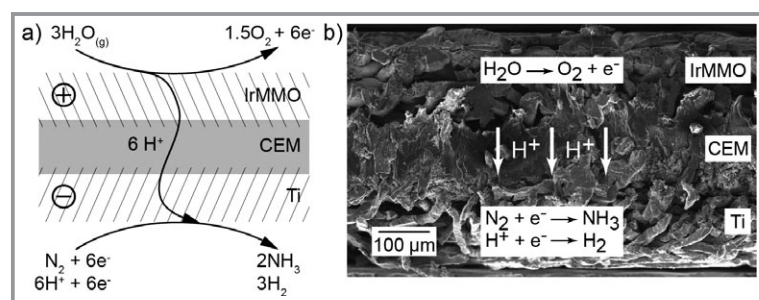
The catalyst used for the N_2 reduction is the most critical component of the MEA. Skúlason et al. investigated the ability of transition metals, such as Ti, for the electrochemical synthesis of NH_3 by density functional theory (DFT) calculations. Titanium mainly adsorbs *N instead of *H. The formation of NH_3 should be the predominant cathodic reaction [17], particularly because the overpotential for the HER on Ti is high [18].

There are four different reaction mechanisms possible for the electrochemical reduction of N_2 to form NH_3: both an associative and dissociative Tafel-type and Heyrovsky-type mechanism [17]. In an associative mechanism adsorbed N_2 adatoms are directly hydrogenated by H^+ at the catalysts surface, while in a dissociative mechanism, N_2 is first dissociated at the catalysts surface and then hydrogenated. In the Tafel-type mechanism, H^+ ions first adsorb at the catalyst's surface and react with electrons to form molecular H_2 adatoms, which then react with adsorbed N_2H_x or NH_x species [19]. In contrast, in the Heyrovsky mechanism, the adsorbed N_2H_x or NH_x species are hydrogenated directly by the attachment of H^+ and electrons [20]. The activation barrier for the Tafel-type mechanism is relatively high (in the range of $1\,eV$) for most transition metal catalysts applied in low-temperature applications and the reaction rate will be slow. The dissociative Heyrovsky mechanism is more likely to occur for early transition metals with flat surfaces such as Ti, Sc, Y, or Zr. The detailed reaction equations can be found in the work of Skúlason et al. [17]

1.2 Co-generation of NH_3 and H_2

The electrochemical synthesis of NH_3 has attracted increased research interest [8]. Lan et al. reported the synthesis of NH_3 from air and liquid H_2O at ambient conditions using an MEA with two Pt/C electrodes and a Nafion 211 membrane. The viable production rates were approximately $1.1 \cdot 10^{-9}\,mol\,s^{-1}cm^{-2}$ after 1 h of experiment. However, the current efficiency was only about 0.5 %. [13]

Recently, Chen et al. also reported NH_3 synthesis using $N_{2(g)}$ at the cathode and a liquid electrolyte at the anode at ambient conditions. At the cathode, a Fe_2O_3-CNT based electrocatalyst was applied. A rate of ammonia formation of $2.2 \cdot 10^{-3}\,g\,m^{-2}h^{-1}$ was achieved. [21]

A distinctive and novel difference of our ecMR was the control of the H_2O activity on the anode side. While Lan et al. and Chen et al. used liquid H_2O, wherein the chemical potential could only be varied by temperature, we used gaseous H_2O, wherein the chemical potential could be changed by varying the degree of saturation.

Recently, Renner et al. published the first alkaline exchange membrane (AEM)-based ammonia production cell at low temperature and low pressure [22]. The feed gas stream was humidi-

Figure 1. a) Visualization of reactions at the MEA: at the anode, H_2O is oxidized to form O_2 and electrons, H^+ migrates through the CEM to the cathode where it combines to H_2 or N_2 is reduced to NH_3. b) SEM image of the MEA consisting of an IrMMO anode, the CEM and a Ti cathode.

fied air, which was fed to the cathode. Here, N_2 and water combine with electrons to form hydroxide and NH_3. The hydroxide ions were transported through the AEM where the ions form O_2 and water. At the cathode Fe, Ni and Fe-Ni nanoparticles over Pt black were investigated as catalyst. The ammonia production rate was $1.33 \cdot 10^{-12}$–$3.80 \cdot 10^{-12}$ mol s^{-1}cm^{-2} [22]. An intensive catalyst preparation and the use of Pt result in higher costs compared to our titanium cathode.

The works published by Skodra et al. [23] and Licht et al. [24] also varied the partial pressure of H_2O used as abundant H_2 source. However, in both publications high temperatures in the range of 200 to 700 °C and more complex electrolyte systems such as a strontian-ceria-ytterbia perovskite disk of the form $SrCe_{0.95}Yb_{0.05}O_{3-\alpha}$ [23] or a molten hydroxide suspension with a molar ratio of 0.5 NaOH/0.5 KOH were applied [24]. The use of high temperatures (500–650 °C) and perovskites was recently reported by Kosaka et al. [25]. Qing et al. reported the ammonia synthesis from 30 % humidified argon and N_2 using a $CsH_5(PO_4)_2/SiO_2$ composite as electrolyte allowing the usage in the intermediate temperature range with high proton conductivity. At a potential of 1.2 V the maximum ammonia formation rate of $2.0 \cdot 10^{-10}$ mol cm^{-2}s^{-1} and a faradaic efficiency of 2.1 % were achieved at 220 °C and atmospheric pressure [26].

The control of the H_2O activity is an essential element of the new ecMR process. Using this additional degree of freedom as a process variable, one can systematically study the influences of the temperature, the relative humidity (RH) of the anode feed stream and the applied cell potential on the NH_3 production rate and the current efficiency. These parameters are also crucial for the stability of the reactor system concerning water management as indicated being important for the operation of fuel cell systems [27]. The ecMR was operated with an Ar feed to the anode with varying amounts of H_2O vapor. Helium or N_2 was fed as the cathodic reactant, and current-voltage curves were recorded. Their time dependence at different process conditions is visualized in the Supporting Information (SI). Helium was used as an inert reference gas to quantify the degree of H_2 production from H^+. Nitrogen as the cathode feed led to NH_3 production as quantified in the Berthelot analysis of the reactor off-gas. As explained beforehand, the electrochemical synthesis of NH_3 comprises two half-cell reactions. At the anode, H_2O is oxidized:

$$3H_2O \rightarrow 6H^+ + 6e^- + 1.5O_2 \quad E_A^0 = 1.228V \quad (1)$$
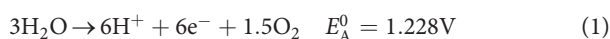
At the cathode N_2 is reduced to NH_3:

$$N_2 + 6H^+ + 6e^- \rightarrow 2NH_3 \quad E_C^0 = -0.057V \quad (2)$$

Under ideal reaction conditions, the minimum cell voltage for the electrochemical synthesis of NH_3 was equal to

$$U_{cell,min} = E_C^0 - E_A^0 = -0.057V - 1.228V = -1.285V \ [28]$$
$$(3)$$

Since the calculated value for $U_{cell,min}$ is only a lower boundary, the minor influence of the pH value and the temperature on the standard potentials were not considered. The anodic and cathodic reactions were kinetically limited and additional overpotentials were observed. No significant electrical current values emerged at potentials below –1.7 V, which was consistent with the high overpotential of Ti for the HER. In fact, this high overpotential for the HER may tailor the ratio of NH_3 and H_2 production rates.

2   Materials and Methods

The MEA was prepared by hot-pressing a H^+-conductive polymer membrane (FuMA-Tech GmbH, Bietigheim-Bissingen, Germany, Fumapem F-14100) between a Ti felt (NV Bekaert SA, Kortrijk, Belgium, fiber diameter 15 μm, porosity 40 %, thickness 100 μm, diameter 50 mm) and a IrMMO felt at 7.5 kN cm^{-2} and 90 °C for 20 min, followed by cooling at the same pressure for 1 min. The IrMMO catalyst was coated by Magneto Special Anodes B.V., Schiedam, The Netherlands, on the Ti felts by the paint-thermal decomposition method. Iridium and tantalum salts were dissolved in butanol. The prepared ink was paint-brushed on the Ti felts in layers of approx. 0.5 g_{metal}m^{-2}. After 10 min drying, the coated felts were decomposed for 20 min at 500 °C to develop the desired catalyst layer on top of the Ti surface.

Before hot-pressing, the membrane was pretreated in an aqueous 10-wt % HNO_3 solution for 3 h at 80 °C, followed by a 1-h treatment in demineralized H_2O at 80 °C. Subsequently, the membrane was NH_4^+-modified to avoid the dissolution of NH_3 in the membrane [13]. The membrane was stored in a 30-wt % NH_4OH solution for 18 h at room temperature, followed by rinsing with demineralized H_2O for six days. The pH of the modified membrane is around 5. Normally, at this pH value and an assumed anodic potential of 1.5 V, the applied anode catalyst IrMMO starts to dissolve [28]. However, H^+ ions are produced by the oxygen evolution reaction at the anode, and thus, the pH value decreases at the membrane/catalyst interface. At a potential of 1.5 V IrO_2 is stable at pH values below 5. Future experiments are necessary to determine the long-term performance of the membrane/catalyst system. From our current experience, the IrMMO seems to be stable under the investigated reaction conditions.

The MEA was placed between two Ti half-cells with a milled-in serpentine flow field. Before the first experiment, the MEA was flushed with inert gas for 2 h to ensure that only the produced NH_3 was analyzed. The cathodic product stream was collected in two consecutive beakers filled with 0.5 M H_2SO_4. The NH_4^+ concentrations were determined three times with a variation of the Berthelot reaction [29].

Polarization curves and chronoamperometry measurements were conducted with a potentiostat (Metrohm

GmbH & Co. KG, Filderstadt, Germany, PGSTAT302N). For further information and the flow chart, see the SI.

3 Results and Discussion

Current-voltage curves were recorded at 30, 50 and 70 °C with varying relative Ar humidity of 25, 50 and 95 % at 1 barg. The corresponding values in mg H_2O per hour and the partial pressure in kPa are given in the SI. The flow rate of all gases applied was 50 mL min^{-1} constantly. The cell potential ranged from –1.7 to –2.5 V with a potential sweep rate of 0.1 V h^{-1}. The obtained current-voltage curves at high temperatures (70 °C at 50 and 95 % RH; and 50 °C at 95 % RH) showed severe current instabilities at higher potentials that were likely due to unstable water management at the anode side similar to those observed in H_2 fuel cells [16]. Due to this unstable system behavior, only the results for 30 °C (all RH) and 50 °C (25 and 50 % RH) are shown (Fig. 2a and 2b).

Higher anodic pressure can be useful to stabilize the system since at higher total pressure the partial pressure of H_2O needs to be reduced to keep the relative humidity constant. However, at higher anodic pressure the risk of membrane dry-out is rising.

Two parameters were of interest to evaluate the results obtained here: a) the NH_3 production rate in mol NH_3 produced per second of experimental time and cm^2 catalyst area perpendicular to the ionic flux and b) the NH_3-specific current efficiency CE_{NH3}, which gives the share of the total charge C transported compared with the amount of NH_3 synthesized (Eq. (4)).

$$CE_{NH3} = \frac{m_{NH3}zF}{M_{NH3}C_{corr}} = \frac{m_{NH3}zF}{M_{NH3}(C_{N2} - C_{He})} \qquad (4)$$

For the co-generation, this number can vary between 0 and 100 % but should be as high as possible if NH_3 is the desired product. In Tab. 1, the production rate and the CE_{NH3} are given.

In Eq. (4), z is the number of electrons needed to form one molecule of NH_3 ($z = 3$), F is Faraday's constant equal to 96 485 C mol^{-1}, and m_{NH3} and M_{NH3} are the mass and the molar mass of NH_3, respectively. The charge $C_{N2/He}$ is the measured average current multiplied by the experimental time. To calculate an NH_3-specific CE (Tab. 1), the H_2 production was determined by reference measurements with He. Measurements with N_2 resulted in H_2 and NH_3 production (m_{NH3}), the latter measured and quantified by the Berthelot reaction. Fig. 2c shows two polarization curve progressions recorded for N_2 and He at the same reaction conditions. The use of N_2 resulted in higher currents compared with the use of He. The produced NH_3 can be quantitatively analyzed in the off-gas. By subtracting the charge C_{He} measured for He, i.e., for the HER, from the charge C_{N2} measured for N_2, i.e., for the formation of NH_3, a corrected
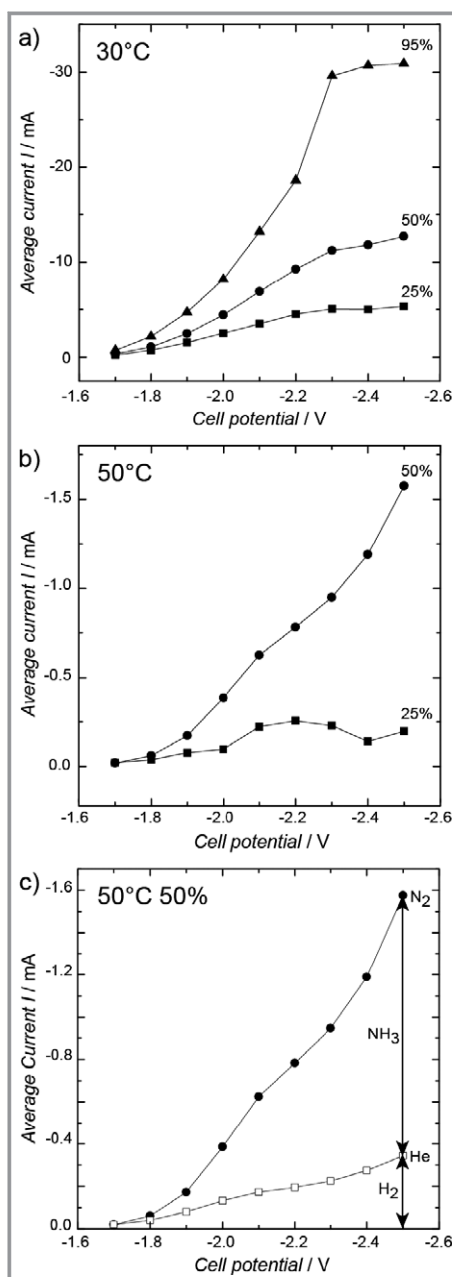

Figure 2. a) Current voltage curves for 25/50 and 95 % RH at 30 °C and b) at 50 °C for 25 and 50 % RH. Currents were averaged for each potential step applied. c) Determination of a corrected charge C_{corr} to calculate a NH_3-specific current efficiency.

current efficiency CE_{NH3} specific for NH_3 synthesis was determined using Eq. (4).

For a N_2 feed, Figs. 2a and 2b show that the measured current increased with the RH and the applied potential. At 30 °C and –2.3 V, a leveling off was observed, and the current increase was less pronounced. This intermediate limiting current was established above –2.5 V, but at even higher current values the HER was predominant and the current increased (data not shown). For 50 °C, the measured current was one magnitude smaller than for 30 °C. This result

Table 1. Maximum average current, integral NH_3 production rates, average power density and integral NH_3 specific current efficiencies (*CE*) determined over whole polarization curves.

| T [°C]	RH [%]	I_{max} [mA]	Production rate [10^{-12} mol s^{-1}cm^{-2}]	Average power density [mW cm^{-2}]	NH_3-specific *CE* [%]
30	25	5.0	0.74	0.40	0.14
30	50	12.0	2.7	0.80	0.23
30	95	30.0	53	1.80	2.13
50	25	0.2	2.5	0.02	8.98
50	50	1.6	4.1	0.08	2.25

was unexpected and cannot be explained at present. Higher current values were expected due to the increased conductivity for H$^+$ and higher reaction rates at the cathode and anode. More H$_2$O was also supplied when compared to the same RH at 30 °C. Tab. 1 provides the maximum currents (I_{max}) and the achieved NH$_3$ production rates for the recorded polarization curves. The phenomenon of decreased current at 50 °C compared to the measurements at 30 °C was also observed when measuring with He instead of N$_2$. The total charge passed during a current voltage-curve recorded from –1.7 V to –2.5 V at 25 % RH was five times lower for 50 °C compared to 30 °C. At 50 % RH the current at 50 °C was even 22 times lower compared to 30 °C. The kinetics of the HER usually gives higher H$_2$ evolution rates with increasing temperature. Due to the complex structure of the MEA the temperature and relative humidity dependency of the achieved current-voltage characteristics need further analysis. The fundamental comprehensive understanding of the system and reactions taking place requires separate studies of the anodic catalyst, the membrane and the cathodic catalyst in experiments where only the cathode or the anode is combined with the membrane and the counter electrode is a well-known system positioned in an H-cell for instance. Electrochemical impedance spectroscopy (EIS) measurements can help to further evaluate the reaction behavior of the applied reactor and MEA system. However, it is beyond the scope of this work to focus on EIS measurements.

The production rates increased with the RH and temperature. However, higher currents did not necessarily result in higher NH$_3$ production rates but may have favored the co-generation of H$_2$. The highest NH$_3$ production rate of $53 \cdot 10^{-12}$ mol s^{-1}cm^{-2} was achieved at 30 °C, 95 % RH and a power density of 1.8 mW cm^{-2}. The power density was similar to the values observed in conventional industrial PEM and alkaline electrolyzers. Unlike fuel cells, ecMRs minimize the power densities by achieving maximum gas production rates: this maximizes the NH$_3$-specific current efficiency CE_{NH3}.

For the integral current efficiency, the NH$_3$ produced was quantified by the Berthelot reaction after a complete polarization curve was measured over 9 h. A maximum value of approx. 9 % at 50 °C and 25 % RH was observed.

Additional current-voltage curves were recorded at 25 % RH with varying temperature from 30 to 70 °C (data not shown). The production rates increased with temperature up to 60 °C. The difference in the production rates between 50 and 60 °C was negligible but the CE_{NH3} was approx. 3.5 times higher at 50 °C.

The following experiments were conducted at 50 °C. To precisely quantify the NH$_3$-specific production rates, hour-long chronoamperometry (CA) measurements were performed at a constant reactor temperature of 50 °C and 7.5, 15 and 25 % RH. For potentials of –1.8 to –2.3 V, the achieved production rates are shown in Fig. 3. At low voltages and high humidity, the current reactor system and the
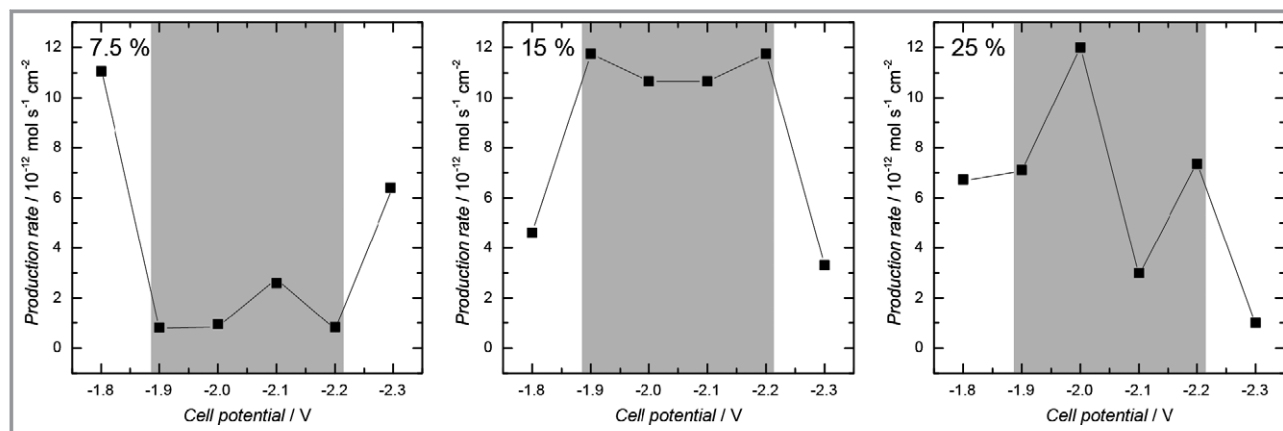
Figure 3. Production rates determined from Berthelot reactions after 1-h chronoamperometry at 7.5, 15 and 25 % RH at 50 °C.

MEA architecture caused instabilities in the process behavior and required optimization, as has been observed in fuel cell systems for the past twenty years.

For 7.5 and 15% RH, approximately constant production rates were observed between cell potentials of –1.9 and –2.2 V. However, at 15 % RH, the values were about ten times higher at an average of $11.5 \cdot 10^{-12} \, \text{mol s}^{-1} \text{cm}^{-2}$. At 7.5 % RH, the system was at its lower operating limit. At these operating conditions, membrane dry-out and fluctuations in the H_2O supply of the liquid flow meter could occur. At 25 % RH, the electrochemical system (MEA) was as such unstable, and in the optimal potential range of –1.9 to –2.2 V no constant production rates were obtained. The achieved CE_{NH3} for the potential range at –1.8 to –2.3 V confirmed this observation (Tab. 2). The most stable and highest CE_{NH3} were reached for 15 % RH and cell potentials of –1.9 to –2.2 V.

The CE_{NH3} for 15 % RH were very stable in the potential range from –1.9 to –2.2 V, and the same production rate of $12 \cdot 10^{-12} \, \text{mol s}^{-1} \text{cm}^{-2}$ was achieved. The CE_{NH3} at –2.2 V was the highest (27.5 %) for a power density of $0.05 \, \text{mW cm}^{-2}$, which is by far smaller than for conventional alkaline electrolyzer or PEM electrolyzer usually showing a power density of $< 1 \, \text{mW cm}^{-2}$ or $< 4.4 \, \text{mW cm}^{-2}$, respectively [7]. The ratio of the integral charges C_{N2}/C_{He} was greater than one indicating that more NH_3 was produced than H_2. Overall, the optimal process conditions were at 50 °C and 15 % RH at an applied potential range of –1.9 to –2.2 V. The highest production rate and the CE_{NH3} were observed in this potential range during CA measurements. However, membrane dry-out at a RH below 25 % has to be considered for future long-term stability tests.

The presented results describe a successful electrochemical N_2 reduction to NH_3 in an ecMR. Titanium was shown as a potential cathodic catalyst for a high NH_3-specific CE. However, the HER remains the dominant parallel reaction.

In comparison to the works published by Lan et al. [13], Skodra et al. [23], Licht et al. [24], and Chen et al. [21], this work demonstrates an easy and at the same time highly efficient process for the electrochemical NH_3 synthesis. The introduced MEA and ecMR system have several advantages compared to reaction systems used in literature so far. The used MEA shows high chemical and mechanical stability. The setup is easy to handle, and alternative catalyst systems can be tested under similar reaction conditions. The possibility to perform measurements either with He or N_2 adds an additional parameter to evaluate the achieved results. Concerning the reaction conditions our system is the most sustainable and environmentally friendly one. The reaction temperature is kept below 100 °C resulting in low costs for thermal energy. Additionally, the system is operated at ambient pressure. Contrary, the system of Licht et al. is operated at 200 °C and the setup of Skodra et al. even at temperatures between 500 and 700 °C. Indeed, Lan et al. operate their system also at temperatures below 100 °C and ambient pressure, but their applied catalyst Pt/C is by far more expensive than the Ti catalyst applied in our MEA. In contrast to Lan et al. and Chen et al., we used gaseous H_2O wherein the chemical potential could be changed by varying the degree of saturation.

Concerning production rate and current efficiency, the current MEA and ecMR system can compete with the systems presented in the literature. The maximum production rate of $2.4 \cdot 10^{-9} \, \text{mol s}^{-1} \text{cm}^{-2}$ reached by Licht et al. is around 200 times higher than the maximum production rate reported here. However, the system was operated at 200 °C at a power density of $2.4 \, \text{mW cm}^{-2}$ compared to $0.05 \, \text{mW cm}^{-2}$ for our work. When introducing a normalized production rate concerning the power density with the unit $\text{mol s}^{-1} \text{mW}^{-1}$, the production rate reached by Licht et al. is only four times higher. The current efficiency of 22 % reached by Licht et al. is in the same order of magnitude as the value reached here, which is 27.5 %. In contrast, Lan et al. could only reach current efficiencies of less than 1 %.

4   Conclusions and Outlook

The presented MEA and ecMR system uses abundant reactants such as H_2O and N_2. The applied cathodic Ti catalyst is cheap and available in many modifications such as felts,

Table 2. NH_3-specific current efficiencies and the ratio for the measured C_{N2} and C_{He} after 1-h chronoamperometry at 7.5, 15 and 25 % relative humidity at 50 °C.

Potential [V]	Relative humidity [%]					
	7.5		15		25	
	CE_{NH3} [%]	C_{N2}/C_{He} [–]	CE_{NH3} [%]	C_{N2}/C_{He} [–]	CE_{NH3} [%]	C_{N2}/C_{He} [–]
–1.9	6.4	2.2	20.5	4.1	5.9	4.9
–2.0	8.5	1.8	16.3	2.9	7.9	3.4
–2.1	18.3	2.0	17.5	2.7	3.0	2.3
–2.2	8.8	1.5	27.5	2.1	18.3	1.5
–2.3	34.0	2.1	9.8	1.9	0.6	2.9

plates or powders. Furthermore, complex electrolytes such as molten salts, which are difficult to handle and need higher reaction temperatures, were not applied.

This work encourages further research on catalysts for the electrochemical synthesis of NH_3 to make the process more efficient in terms of NH_3 selectivity and production rates. There are several ways to improve the achieved production rate and current efficiency of the ecMR. First of all, the specific surface area of the applied catalysts needs to be increased. For that reason, particle synthesis of proper electrocatalysts needs to be considered to replace the randomly structured metal felts applied in the present work by catalyst powders. The design and the preparation of the MEA need to be adjusted accordingly to maintain mechanical stability. Another advantage of applying catalyst particles instead of catalyst felts is that the ratio of, e.g., two components of a binary catalyst can easily be changed and, thus, the properties of the investigated catalyst.

In another approach, the type and, therefore, the properties of the applied membrane can be modified. One possibility is the use of polybenzimidazole (PBI) membranes instead of polytetrafluoroethylene(PTFE)-based cation exchange membranes. Since PBI membranes show H^+ conductivity without H_2O needed for the transport mechanism, problems related to flooding of the cathodic department or blocking of active sites of the cathodic catalyst can be reduced. However, PBI membranes require pretreatment with phosphoric acid, to which Ti is not corrosion resistant. Thus, either the cell design or the cell material needs to be improved. Finally, the cathodic catalyst can be further optimized, or different morphologies of the applied Ti catalyst have to be tested to increase the triple phase boundary between catalyst, membrane and the gaseous reactants. Other catalysts such as Ag or Pd, for which studies in the literature show high activity, can be tested as well. These catalysts, of course, would increase the material costs compared to Ti. Nevertheless, the results obtained in the present work are very promising to encourage further investigation and optimization of the applied Ti catalysts.

From an experimental point of view, the optimal process parameters can further be narrowed down. Additionally, further aspects such as the application of higher pressure both at the anode and at the cathode and the pressure ratio between the anodic and the cathodic pressure can be considered as well.

Symbols used

C	[C]	charge
CE	[%]	current efficiency
E^0	[V]	standard electrode potential
F	[C mol^{-1}]	Faraday's constant
I	[A]	current
m	[g]	mass
M	[g mol^{-1}]	molar mass
U	[V]	cell voltage
z	[–]	number of electrons

Sub- and Superscripts

A	anode
C	cathode
corr	corrected
max	maximum
min	minimum

Abbreviations

AEM	alkaline exchange membrane
CA	chronoamperometry
CEM	cation exchange membrane
DFT	density functional theory
ecMR	electrochemical membrane reactor
EIS	electrochemical impedance spectroscopy
HER	hydrogen evolution reaction
IrMMO	iridium mixed metal oxide
MEA	membrane electrode assembly
OER	oxygen evolution reaction
PBI	polybenzimidazole
PEM	proton exchange membrane
PTFE	polytetrafluoroethylene
RH	relative humidity

References

[1] V. Smil, *Nature* **1999**, *400*, 415.

[2] I. Rafiqul, C. Weber, B. Lehmann, A. Voss, *Energy* **2005**, *30 (13)*, 2487–2504. DOI: https://doi.org/10.1016/j.energy.2004.12.004

[3] G. Wang, A. Mitsos, W. Marquardt, *AlChE J.* **2017**, *63 (5)*, 1620–1637.

[4] C. Zamfirescu, I. Dincer, *J. Power Sources* **2008**, *185 (1)*, 459–465. DOI: https://doi.org/10.1016/j.jpowsour.2008.02.097

[5] R. Lan, J. T. S. Irvine, S. Tao, *Int. J. Hydrogen Energy* **2012**, *37 (2)*, 1482–1494. DOI: https://doi.org/10.1016/j.ijhydene.2011.10.004

[6] R. Lan, S. Tao, *ECS Electrochem. Lett.* **2013**, *2 (5)*, F37–F40. DOI: https://doi.org/10.1149/2.007305eel

[7] M. Carmo, D. L. Fritz, J. Mergel, D. Stolten, *Int. J. Hydrogen Energy* **2013**, *38 (12)*, 4901–4934. DOI: https://doi.org/10.1016/j.ijhydene.2013.01.151

[8] S. Giddey, S. P. S. Badwal, A. Kulkarni, *Int. J. Hydrogen Energy* **2013**, *38 (34)*, 14576–14594. DOI: https://doi.org/10.1016/j.ijhydene.2013.09.054

[9] K. Kugler, B. Ohs, M. Scholz, M. Wessling, *Phys. Chem. Chem. Phys.* **2014**, *16 (13)*, 6129. DOI: https://doi.org/10.1039/c4cp00173g

[10] S. M. A. Kriescher et al., *Electrochem. Commun.* **2015**, *50*, 64–68. DOI: https://doi.org/10.1016/j.elecom.2014.11.014

[11] J. Nash et al., *J. Electrochem. Soc.* **2017**, *164 (14)*, F1712–F1716.

[12] X. Yang et al., *J. Am. Chem. Soc.* **2018**, *140 (41)*, 13387–13391. DOI: https://doi.org/10.1021/jacs.8b08379

[13] R. Lan, J. T. S. Irvine, S. Tao, *Sci. Rep.* **2013**, *3*, 1145. DOI: https://doi.org/10.1038/srep01145

[14] C. Comninellis, G. P. Vercesi, *J. Appl. Electrochem.* **1991**, *21*, 335–345.

[15] P. Choi, N. H. Jalani, R. Datta, *J. Electrochem. Soc.* **2005**, *152 (3)*, E123. DOI: https://doi.org/10.1149/1.1859814

[16] T. V. Nguyen, R. E. White, *J. Electrochem. Soc.* **1993**, *140*, 2178–2186.

[17] E. Skúlason et al., *Phys. Chem. Chem. Phys.* **2012**, *14 (3)*, 1235–1245. DOI: https://doi.org/10.1039/c1cp22271f

[18] S. Trasatti, *J. Electroanal. Chem.* **1972**, *39*, 163–184.

[19] J. Tafel, *Z. Phys. Chem., Stoechiom. Verwandtschaftsl.* **1905**, *50*, 641–712.

[20] J. Heyrovsky, *Recl. Trav. Chim. Pays-Bas* **1927**, *46*, 582–585.

[21] S. Chen, S. Perathoner, C. Ampelli, C. Mebrahtu, D. Su, G. Centi, *Angew. Chem.* **2017**, *129*, 2743–2747.

[22] J. N. Renner, L. F. Greenlee, A. M. Herring, K. E. Ayers, *Electrochem. Soc. Interface* **2015**, 51–57.

[23] A. Skodra, M. Stoukides, *Solid State Ionics* **2009**, *180 (23–25)*, 1332–1336. DOI: https://doi.org/10.1016/j.ssi.2009.08.001

[24] S. Licht et al., *Science* **2014**, *345 (6197)*, 637–640. DOI: https://doi.org/10.1126/science.1254234

[25] F. Kosaka, T. Nakamura, A. Oikawa, J. Otomo, *ACS Sustainable Chem. Eng.* **2017**, *5 (11)*, 10439–10446. DOI: https://doi.org/10.1021/acssuschemeng.7b02469

[26] G. Qing, R. Kikuchi, S. Kishira, A. Takagaki, T. Sugawara, S. T. Oyamaa, *J. Electrochem. Soc.* **2016**, *163 (10)*, E282–E287. DOI: https://doi.org/10.1149/2.0161610jes

[27] M. Ji, Z. Wei, *Energies* **2009**, *2*, 1057–1106.

[28] M. Pourbaix, *Atlas of Electrochemical Eyuilibria in Aqueous Solutions*, NACE International Cebelcor, **1974**.

[29] R. B. Willis, M. E. Montgomery, P. R. Allen, *J. Agric. Food Chem.* **1996**, *44*, 1804–1807.